ACADEMIA ROMÂNĂ
Revue Roumaine de Chimie
http://web.icf.ro/rrch/

Rev. Roum. Chim.,
2013, *58*(2-3), 229-238

Dedicated to Professor Bogdan C. Simionescu
on the occasion of his 65th anniversary

MOLECULAR DYNAMICS EVALUATION OF HYALURONAN INTERACTIONS WITH DIMETHYLSILANEDIOL IN AQUEOUS SOLUTION

Daniela IVANOV[a,b] and Andrei NEAMTU[a,c*]

[a] "Petru Poni" Institute of Macromolecular Chemistry, 41A Gr. Ghica Voda Alley, 700487 Iaşi, Roumania
[b] Department of Natural and Synthetic Polymers, "Gh. Asachi" Faculty of Chemical Engineering and Environmental Protection Technical University of Iaşi, 700050 Iaşi, Roumania
[c] Center for the Study and Therapy of Pain (CSTD), "Gr. T. Popa" University of Medicine and Pharmacy, 16, University Street, 700115, Iaşi, Roumania

Received November 29, 2012

Molecular dynamics simulations (MD) were performed on hexasaccharide hyaluronan (HA) models in both absence and presence of dimethylsilanediol (DMSD) and in explicit aqueous/sodium ions solvent that mimic physiological solutions. The advantage of the simulation as an investigation technique to describe the physical bonding of DMSD to HA is of great importance as it considers simultaneously all the interactions among the component species and it also counts on the entropic effects. We found that the hydrogen bonding of DMSD to HA is slightly stronger than for water but comparable to it and DMSD did not affect the global water pattern around the HA oligosaccharides. On the other hand the HB self-interactions in HA were not influenced by the DMSD molecules in solution, despite their particular affinity for the carboxylate of GlcUA and –CH2–OH of GlcNAc groups. Free energy landscapes for the β(1→3) and β(1→4) glycosidic bond confirmed that the conformation of HA oligosaccharides was preserved in the presence of DMSD for the time frame followed during simulations. Moreover, the conformations of HA generated from the minimum energy glycosidic dihedrals in the absence (MD) and in the presence of DMSD (MD-DMSD) compared to the experimental models from database (Protein Data Bank) could be placed between a fourfold and a threefold periodicity, but closer to the three fold form.

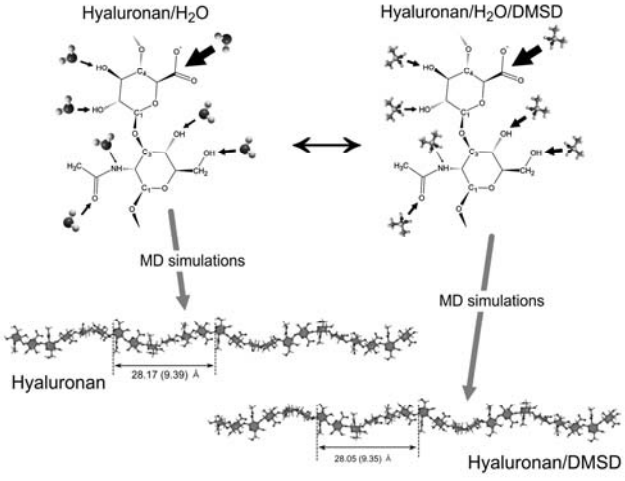

INTRODUCTION

A variety of hydrogels are being employed as scaffold materials. They are composed of hydrophilic polymer chains, preferable natural in origin and may present mechanical and structural properties similar to the tissues and the ECM. The structural integrity of the generated hydrogels depends on crosslinks between polymer chains *via* various chemical bonds and physical interactions.

* Corresponding author: neamtuandrei@gmail.com

Hyaluronic acid (Fig. 1), a natural polymer, plays an essential role in many biological processes such as tissue hydration, nutrient diffusion, proteoglycan organization, and cell differentiation. Moreover, oligomers represented entities able to activate the immune cells and to deliver endogenous signals with respect to stress, but also to be powerful inducers of inflammation and angiogenesis.[1,2]

Due to its excellent biocompatibility, biodegradability, as well as excellent gel-forming properties, HA and its derivatives have been widely explored as hydrogels for tissue engineering. It is the only nonsulfated glycosaminoglycan in the extracellular matrix. HA is medically important, in pure form being non-immunogenic, having unique viscoelastic properties and exhibiting pivotal roles in cell differentiation and cell motility.[3]

HA self-association, electrostatic repulsion between individual HA polymers, combined with extensive hydration of the polymers, confers a viscous, gel-like property to aqueous solutions of HA. The behavior of HA in solutions even at low concentration is far from ideal Newtonian. HA, which behaved as a stiffened random coil in solution, occupies a large hydrated volume and therefore showed solute-solute interactions at unusually low concentration. In a physiological solution, the backbone of a HA molecule is stiffened by a combination of the chemical structure of the disaccharide, internal hydrogen bonds, and interactions with solvent. The axial hydrogen atoms form a non-polar, relatively hydrophobic face while the equatorial side chains form a more polar, hydrophilic face, thereby creating a twisting ribbon structure.[4,5] HA in solution assumes a stiffened helical configuration, which can be attributed to hydrogen bonding between the hydroxyl groups along the chain. As a result, a coil structure is formed that traps approximately 1000 times its weight in water.[6]

There is an increasing interest, especially for the companies, to use hyaluronic acid in association with silanediols such dimethilsilanediol or methylsilanetriol. Silanediols may have advantages because they are stable to dehydration and are neutral at physiological pH.[7]

Geminal silanediols, in addition to their well-known role as precursors to organosilicon polymeric materials, in the last few years have attracted the attention of biochemists as protease inhibitors.[8-10] The inhibition process occurs via the establishment of hydrogen bonds between the inhibitors and the active site of the enzyme or the quelation of the metallic center, the structure of the $Si(OH)_2$ group seems to play an important role in their biological activity.[11] Moreover, silanols present biocides properties, demonstrated an enhanced antimicrobial activity compared to the analogous organic alcohols, probably due to a greater acidity compared to the corresponding organic alcohols because of electron back donation from oxygen through (p→d orbital) π bond.[12]

HA is highly dynamic in aqueous solution and sensitive to the specific ionic conditions. According to simulation data, HA molecules are stiffened by a rapidly interchanging network of transient hydrogen bonds at the local level and do not significantly associate at the global level. Until recently, there was little intuition as to the nature of these interactions and their persistence as compared with intramolecular and intermolecular interactions. MD computational approaches can make more realistic the dynamic simulations of segments of these molecules in the presence of explicit water molecules.

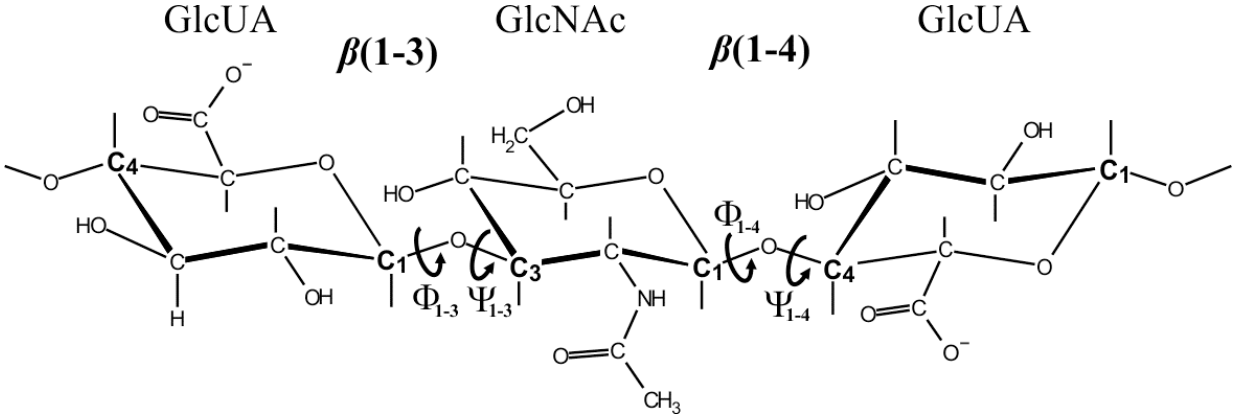

Fig. 1 – HA structure and nomenclature for the glycosidic $\beta(1\rightarrow3)$ and $\beta(1\rightarrow4)$ linkages dihedral angles.

The presence of dimethylsilanediol (DMSD) should not disturb the active sites from HA so the physiological properties would be not affected. The present study represents a theoretical attempt at to understand the nature of interactions between HA chains and dimethylsilanediol from the dynamic molecular viewpoint in water environments, how its three-dimensional dynamic structure arises out of interactions with water in the presence of silanediol compared to intra- and intermolecular self associations in absence of silanediol.

COMPUTATIONAL METHODS

Molecular dynamics (MD) simulations were performed on HA/water systems containing 3 HA molecules randomly placed inside a cubic simulation box and 6727 water molecules. To one system 36 molecules of dimethylsilanediol were added. The simulation results for the two systems were analyzed comparatively. The HA oligomers consisted of three disaccharide units of –GlcUAβ1-3GlcNAcβ1-4 (Figure 1). The energy minimizations, MD simulations and subsequent data analyses were performed with the GROMACS 4.5.4 suite and Glycam force field was used for HA description.[13] For water the TIP4P-EW model[14] was chosed as it is parametrized to be used with Ewald summation techniques for electrostatics.

For dimethylsilanediol the parameters were obtained as follows. The bond, angle and dihedral parameters were taken from the generalized Amber force field (GAFF) by replacing silicone with sp^3 GAFF carbon atom type 'c3'. The bond equilibrium lengths between silicone, oxygen and carbon atoms were modified compared to the GAFF values to account for Si different radius. They were computed from a B3LYP DFT energy minimization run of a dimethylsilanediol molecule. Lenard-Jones parameters for Si (σ = 2.96 Å, ε = 0.879 kJ/mol) were taken from the DOCK 6.5 software suite.[15-17] The atomic partial charges of DMSD were computed by fitting the molecular electrostatic potential computed at HF/6-31G* level of theory. The fitting procedure included two stages with different weighting factors (0.0005/0.001) for the restrained electrostatic potential fit (RESP) procedure.[18] Connolly surface algorithm was used for generating the fitting grid points. The procedure of the charge derivation is similar to the one used for GAFF development. GAFF and Glycam force fields are compatible as they were both developed to be used in conjunction with the Amber force field suite.[19-23] This assures that the HA, dimethylsilanediol and water molecules are described in a consistent manner in the present simulations.

The simulation time for the production run was 50 ns for each system. All the simulations were done at constant temperature and pressure (NPT ensemble). For the pressure, the Berendsen scheme was used with a compressibility of 4.5×10^{-5} (bar^{-1}) and a relaxation time of 1 ps and a reference pressure of 1 atm. V-rescale thermostat[24] was used for temperature coupling at 300 K with a relaxation constant of 0.1 ps. The electrostatic interactions were evaluated using the particle mesh Ewald (PME) summation method.

The free energy plots of the system were computed from the distribution of the system states in the bidimensional space of glycosidic dihedral angles Φ and Ψ by taking the histogram (density of states) and transforming it in accordance with the Boltzmann formula:

$$\Delta G = - k_B T \ln(P_{i,j}/P_{max})$$

where ΔG is the Gibbs free energy difference, k_B is the Boltzmann constant, T is the absolute temperature $P_{i,j}$ is the frequency corresponding to the i,j interval in $\Phi \times \Psi$ plane and P_{max} is the maximum frequency over the entire range of Φ and Ψ dihedral angles.

All the simulations were carried out on a 64 core high performance computing cluster (Dell PowerEdge 1950 servers) at the Molecular Modeling Laboratory, CSTD – "Gr. T. Popa" University of Medicine and Pharmacy, Iaşi.

RESULTS AND DISCUSSION

MD simulations were performed on a hexasaccharides HA model in both absence and presence of dimethylsilanediol (DMSD) and in explicit aqueous/sodium ions solvent that mimic the physiological solutions. Hydrogen bonding plays a major role in the conformation that biological macromolecules adopt in aqueous media. Thus, an intimate interplay arises between the intra-molecular and inter-molecular solvent hydrogen bonding network, this being equally true for proteins, nucleic acids and carbohydrates.[25] The pattern of the hydrogen bond (HB) network developed in solution around a saccharide is dependent not only on the water layers organization

but also on other solute species capable of hydrogen bonds formation or hydrophobic interactions with different groups or surface patches of the polymer chain.[26] Recognizing the importance of the hydrogen bonding on specific HA conformation in the analysed solutions, a statistical evaluation of both inter- and intra-molecular hydrogen bonds was performed.

Table 1 presents the number and the estimated life-times of the hydrogen bonds generated between the dissolved DMSD and representative exocyclic groups of GlcUA and GlcNAc monosaccharide residues. The analysed sites includes the carboxylate group and the hydroxyls in position '2' and '3' of GlcUA and –C=O, –NH, $–CH_2–OH$ and hydroxyl in position '4' of GlcNAc respectively. It was considered that donor-hydrogen-acceptor atom triplets –X–H···Y participate to a hydrogen bond if two geometric criteria were satisfied simultaneously: the distance between the donor 'X' and the acceptor 'Y' was shorter than 0.35 nm (corresponding to the first minimum of the radial distribution function of water) and the angle between the hydrogen 'H' – donor 'X' and acceptor 'Y' was lower than 30°.[27] The system configuration was saved at every 1 ps time interval and the number of hydrogen bonds were determined for the group pairs selected. Its average value was expressed as the number of hydrogen bonds per frame (N_{HB}).

The number of HB/frame in Table 1 shows that the preferred interaction site of DMSD molecule with HA is the carboxylate $–COO^-$ group of GlcUA, nearly 200% more populated than the $–CH_2–OH$ in position '6' and –OH in position '4' of GlcNAc. The hydroxyl groups in positions '2' and '3' on the GlcUA formed a significant smaller number of hydrogen bond interactions with DMSD but comparable with the –C=O group of GlcNAc. By far the less populated site is the –NH of the acetamido group, with almost 10% of the number of hydrogen bonds corresponding to the carboxylate group. The relative propensity of different HA hydrogen bonding sites for DMSD is graphically summarized in the last column of Table 1.

Even the preference of hydrogen bonding species for the $–COO^-$ moiety is somehow expected taking into account its net electrical charge, the DMSD interaction with HA at different sites is not straightforward to predict *a priori* only from the structural formula of HA and DMSD alone. This is due to the competition that arises in the system between different components. Here, the advantage of the simulation as an investigation technique comes into play as it considers simultaneously all the interactions among the component species and it also counts on the entropic effects as well. The bonding of DMSD at various sites along the HA molecule may be 'eclipsed' by the water network developed around the saccharide on one hand and, by the intra-molecular hydrogen bonds of HA on the other hand. Water is known to play an important role in the dynamic structure of oligosaccarides with the first layer of hydration being thought as integral part of the dynamic conformation.[28] Thus, any structural alterations of the bound water layer will have a non-negligible effect on the HA conformation and dynamics.

Table 1

The number of hydrogen bonds and bond lifetimes for the DMSD – HA interaction.
In the last column a graphical representation is given with the arrow widths proportional to the number of hydrogen bonds

Residue	Group	N_{HB}/n_{hb}	τ (ps)	
GlcUA	$– COO^–$	58.6/1.60	39.9	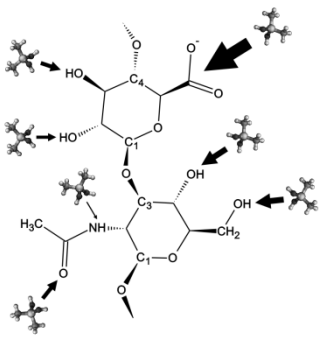
	–OH2	15.1/0.42	7.2	
	–OH3	19.5/0.54	6.1	
GlcNAc	–C=O	19.6/0.54	14.0	
	–NH	5.6/0.15	3.7	
	$–CH_2–OH$	28.9/0.80	11.5	
	–OH4	28.5/0.79	11.9	

N_{HB} – total number of HB / saved frame ($\times 10^{-2}$)
n_{hb} – the number of HB / saved frame / molecule of DMSD ($\times 10^{-2}$)

Table 2

Hydrogen bonds statistics for the water – HA interaction in the presence and in the absence of DMSD. The last column presents graphically the affinity of water to different sites on HA (the arrow widths are proportional to the number of hydrogen bonds)

		Wat – HA		Wat – HA – DMSD		
Residue	**Group**	N_{HB}/n_{hb}	τ (ps)	N_{HB}/n_{hb}	τ (ps)	
GlcUA	– COO^-	3142/0.47	18.8	3105/0.46	20.4	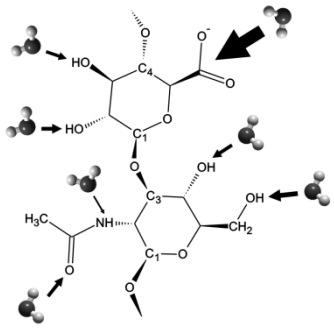
	–OH2	958/0.13	5.3	973/0.14	5.9	
	–OH3	800/0.12	4.1	793/0.12	4.3	
GlcNAc	–C=O	876/0.13	3.6	863/0.13	3.9	
	–NH	425/0.06	2.4	432/0.06	2.7	
	$–CH_2–OH$	1201/0.19	3.7	1203/0.18	3.9	
	–OH4	782/0.12	4.3	763/0.10	4.9	

N_{HB} – total number of HB / saved frame ($\times 10^{-2}$)
n_{hb} – the number of HB / saved frame / molecule of DMSD ($\times 10^{-2}$)

To evaluate the aspect of HB competition the water-HA and the HA-HA hydrogen bonds statistics were performed. For water-HA bonding the results are presented in Table 2. We can see from these data that the number of HB/frame between water and HA exceeds with one or two orders of magnitude the bonding of DMSD at the same sites.

The relative affinity of water for the exocyclic groups of HA follows the same pattern as in DMSD case with the $–COO^-$ of GlcUA being the most populated group, followed in order by the $–CH_2–OH$ of GlcNAc, the hydroxyl groups in position '2' and '3' of GlcUA and the –C=O of GlcNAc. The less affinity is observed for the –NH moiety, similar to the DMSD bonding.

Nonetheless, a more subtle view can be subtracted from the simulations if one computes the number of hydrogen bonds per molecule n_{hb} eliminating in this way the concentration related effects. Notably, the numbers of HB per molecule of DMSD are larger than the corresponding numbers for water-HA interaction (per water molecule), at the same interaction sites. This suggests that the physical bonding of DMSD to HA is slightly stronger than for water but *comparable* to it. However due to the high relative water/DMSD ratio (187:1) (low concentration regime) the effect of DMSD should be minimal on HA as it will become clear in the following from the conformational analysis data.

The HB lifetimes distribution can provide a complementary perspective of hydrogen-bond dynamics in liquid systems.[29,30] It is dependent and, thus gives information, not only on the instantaneous hydrogen bond strength but also on the local molecular structuring and diffusion.[31] The HB lifetime is not easily to asses quantitatively due to the ambiguity in the definition of HB breakage and formation,[27] several approaches being presented in the literature.[32,33] We considered appropriate for the HB kinetics description in the present study the diffusion/exponential decay model of Luzar and Chandler.[34] The resulting lifetimes for DMSD-HA and water-HA interactions are presented in Table 1 and Table 2. It can be seen that the HB lifetimes can be correlated with the number of HB. The longer lifetimes correspond to the $–COO^-$ group in both DMSD and water cases, with higher values for DMSD when compared to water on the same HA side groups. This result is consistent with the higher HB number/molecule found for DMSD.

On the other hand if compare the overall HB numbers and the HB lifetimes for water-HA interaction in the absence and in the presence of DMSD, the results are comparable with no notable differences. This means that at the simulated concentration, despite the affinity of DMSD for several binding sites of HA, the DMSD did not affected the global water HB pattern around the HA oligosaccharides.

One aspect that must be enhanced is the similarity of the hydrogen bonding affinity pattern of DMSD compared to water for HA, which can easily be noticed from the visual inspection of the charts in Table 1 and Table 2. It demonstrates, together with the higher number of HB/molecule in the case of DMSD-HA interaction, that the DMSD molecules can easily interchange with water at the exocyclic groups of HA, process that do not affect the water structuring at low concentrations of DMSD.

Table 3

Hydrogen bonded self-interactions in HA alone and in the presence of DMSD.
The last row presents a diagram with the important sequential HB along the HA chain

β(1→3)					β(1→4)				
H-bond	n_{hb}	n_{hb} +DMSD	τ (ps)	τ (ps) +DMSD	H-bond	n_{hb}	n_{hb} +DMSD	τ (ps)	τ (ps) +DMSD
a	58.8	56.8	8.2	12.2	**d**	124.6	121.7	9.6	11.4
b	0.04	0.06	1.2	1.7	**e**	8.8	9.6	4.3	4.6
c	12.4	13.2	5.4	6.0	**f**	1.1	0.8	0.8	0.7

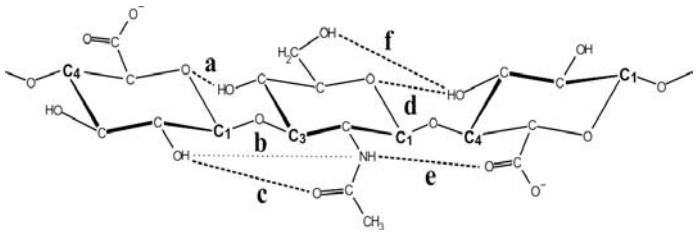

n_{hb} – the number of HB / saved frame / number of HB interacting groups ($\times 10^{-2}$)

Beside the inter-molecular (DMSD-HA and water-HA) HB interactions, of great importance are also the intra-molecular hydrogen bonding patterns of HA itself. The hydrogen bonded self-interactions in HA were quantified and presented in Table 3 along with the influence that DMSD may exert on the number and lifetime of these HB

Four intra-molecular HB were found to be of great importance on the conformation that the $\beta(1\rightarrow3)$ and $\beta(1\rightarrow4)$ glycosidic bonds of HA adopt in solution. These are denoted by '**a', 'c', 'd'** and **'e'** on the diagram depicted in Table 3. The most stable one, the **'d'** bond, formed between the O5 oxygen atom of GlcNAc and the hydroxyl in position '2' of the next GlcUA residue, restricts the conformational range accessible to the $\beta(1\rightarrow3)$ linkage. The **'a'** bond generated between the O5 oxygen atom of GlcUA and the hydroxyl group in position '4' of the following GlcNAc residue is also highly frequent and stabilizes the $\beta(1\rightarrow4)$ glycosidc link. Finally, the **'a'** bond was earlier predicted as being specific for HA but not for chondroitin sulfate due to the axial arrangement of hydroxyl in position '4' of GalNAc.[28]

Two other less persistent HB that alter the flexibility of the glicosidic bridges could be identified in the simulations. The **'c'** bond forms between the –OH in position '2' of GlcUA and the –C=O of the acetamido group of GlcNAc. The **'e'** hydrogen bond link the –NH of the acetamido group and the carboxylate $–COO^-$ of the next GlcUA residue. These two HB are coupled as they both involve the acetamido moiety. It must be stated that beside the direct inter-residue hydrogen bonding involving the acetamido, water bridge interactions with the neighboring groups may be also present.[35] It is not clear however to which extent they influence the conformational behavior of β-linked sugars in contrast to α-linked ones which are more likely to interact via water bridges.[28] These interactions are beyond the aim of the current study and they will not be discussed here.

To asses for the acetamido group orientation relative to the neighboring residues, the –OH2 ··· HN– hydrogen bond was also monitored during the simulations (the **'b'** bond). It is obvious from the data from the Table 3 that this bond is highly disfavored, being characterized by a very low number of HB with shorter lifetime.

Thus, the intra-molecular HB analysis suggests that the conformational motion of the $\beta(1\rightarrow3)$ and $\beta(1\rightarrow4)$ glycosidic linkages is restricted mainly by the stability of the four important sequential H-bonds described above. This is in excellent agreement with other experimental/simulation studies,[36,28] validating in this way the model used in here.

Comparing the results obtained for the pure HA system with the HA/DMSD system it is clear that the HB self-interactions in HA are not affected by the DMSD molecules present in solution, despite their particular affinity for the carboxylate of GlcUA and $–CH_2–OH$ of GlcNAc groups. The number of HB per interacting groups has near the same value for each corresponding pair. The HB lifetimes are longer for the bonds formed between the ring oxygen of one residue and the adjacent –

OH group of the next residue, *i.e.* the **'a'** and **'d'** bonds. The long lifetimes of **'a'** and **'d'** bonds complementary sustain the hypothesis of high stability of these bonds. On contrary, the lifetime of the highly improbable **'b'** bond is an order of magnitude lower compared with the stronger interactions **'a'** and **'d',** which correlates with the number of HB for this bond being under 0.1% from the ones of the **'a'** or **'d'** cases. The unperturbed intra-molecular HB network suggests that the conformational basins explored by the studied oligosaccharides should remain unaffected in the presence of DMSD.

To clearly asses this hypothesis, a conformational analysis was comparatively conducted on the trajectories obtained from the simulations in the absence and in the presence of DMSD. Usually, the conformation of the backbone of carbohydrates is expressed in terms of the Φ and Ψ glycosidic dihedral angles. They give the relative orientation of two adjacent sugar rings and, when plotted against each other in a plane, the coupling between these two angles can identify the conformational basins visited by the saccharide chain. The density of points, each one being defined by a certain (Φ, Ψ) pair, can readily be transformed into a free energy surface by constructing the two dimensional histogram of states and applying the Boltzmann formula as described in the "Methods" section.

The Φ and Ψ angles were defined in accordance with the IUPAC nomenclature: $\Phi_{1\text{-}3}$ ≡ (O5-C1-O3'-C3'), $\Psi_{1\text{-}3}$ ≡ (C1-O3'-C3'-C4') and $\Phi_{1\text{-}4}$ ≡ (O5-C1-O4'-C4'), $\Psi_{1\text{-}4}$ ≡ (C1-O4'-C4'-C5'). The resulting charts are plotted in Fig. 2 for the β(1→3) GlcUA-GlcNAc and in Fig. 3 for the β(1→4) GlcNAc-GlcUA glycosidic bonds.

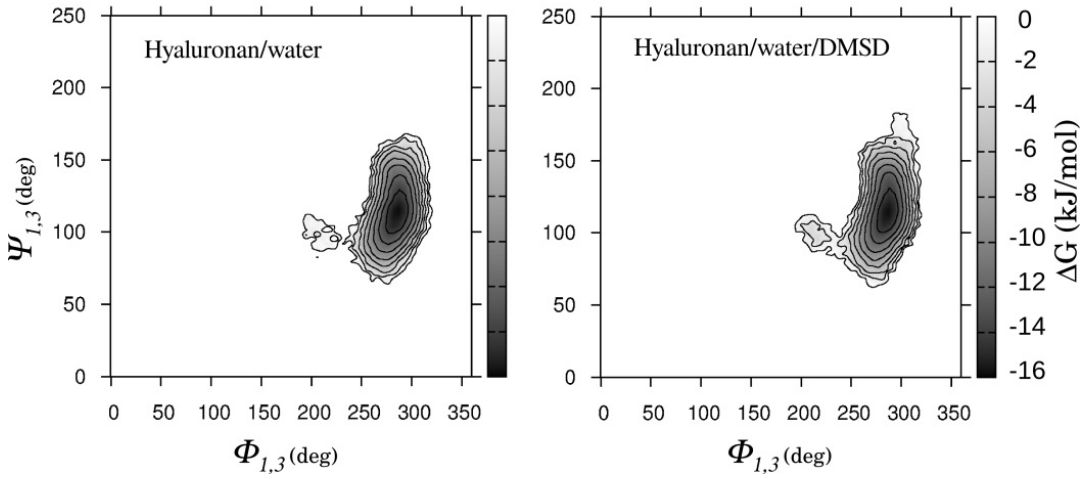

Fig. 2 – Free energy landscapes for the β(1→3) glycosidic bond in the space of dihedral torsional angles (Φ, Ψ) for the HA (left) and HA/DMSD (right) systems.

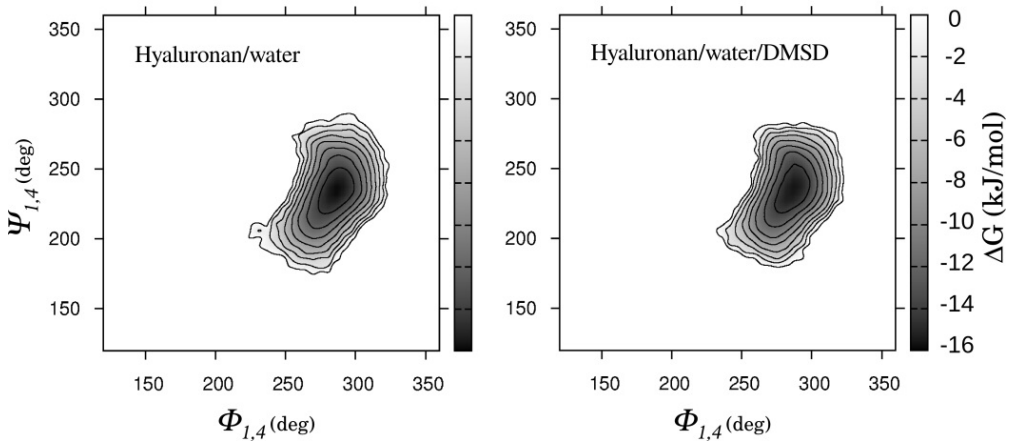

Fig. 3 – Free energy landscapes for the β(1→4) glycosidic bond in the space of dihedral torsional angles (Φ, Ψ) for the HA (left) and HA/DMSD (right) systems.

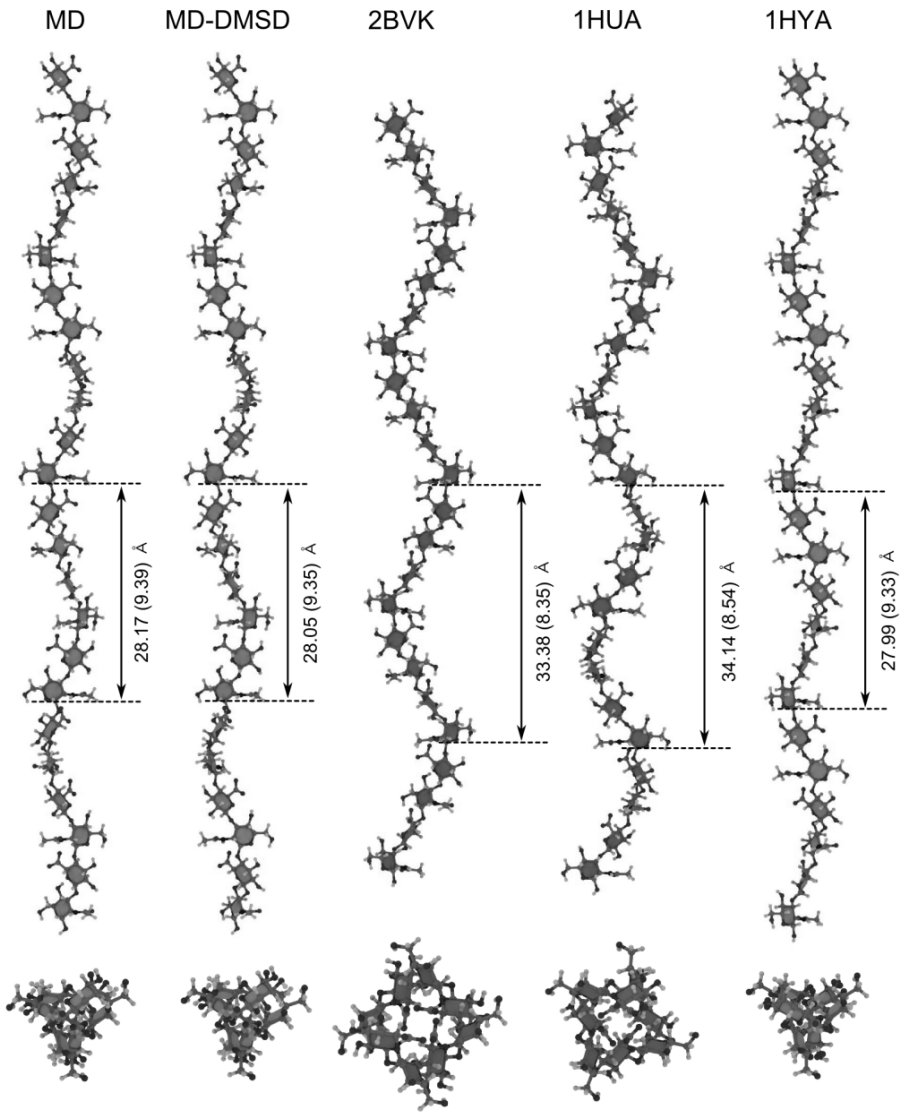

Fig. 4 – Left handed helical models constructed using the minimum energy (Φ, Ψ) dihedral angles obtained from the simulations (MD and MD-DMSD). For comparison three experimental structures from Protein Data Bank (PDB) are given. See text for details.

It can be seen from these charts that the positioning and the 'spatial' extent of the basins explored by the (Φ, Ψ) dihedral angles is identical for the two cases in study, equally true for both the $\beta(1\rightarrow3)$ and $\beta(1\rightarrow4)$ glycosidic linkages. This confirms that the conformation of HA oligosaccharides was not affected by the presence of DMSD for the time frame followed during simulations.

The $\beta(1\rightarrow3)$ glicosidic bond is characterized in both cases by a most probable conformation defined by ($\Phi_{1\text{-}3}$ = 288°, $\Psi_{1\text{-}3}$ = 115°) and the $\beta(1\rightarrow4)$ linkage by ($\Phi_{1\text{-}4}$ = 287°, $\Psi_{1\text{-}4}$ = 237°). These minima are in good agreement with other simulation and experimental NMR and X-ray diffraction data: ($\Phi_{1\text{-}3}$ = 291°, $\Psi_{1\text{-}3}$ =129°; $\Phi_{1\text{-}4}$ = 289°, $\Psi_{1\text{-}4}$ = 247°),[37] ($\Phi_{1\text{-}3}$ = 280°, $\Psi_{1\text{-}3}$ = 134°; $\Phi_{1\text{-}4}$ = 286°, $\Psi_{1\text{-}4}$ = 246°),[38] ($\Phi_{1\text{-}3}$ = 294°, $\Psi_{1\text{-}3}$ = 118°; $\Phi_{1\text{-}4}$ = 277°, $\Psi_{1\text{-}4}$ = 225°).[39]

Using the maximum probability values for the (Φ, Ψ) dihedral angles it was possible to construct extended models of HA composed of more than three disaccharides in order to determine the helical structure of HA predicted by simulation and to compare with experimental reported data. The generated models for HA in the absence (MD) and in the presence of DMSD (MD-DMSD) along constructed models based on the experimental data are presented in Fig. 4.

It is well known that the HA chain adopts left handed helical conformations both in solution and in fiber crystals.[40] These data are consistent with the lowest energy conformations for the linkages found by earlier computer simulations. Here we

found for pure HA solution a minimum energy conformation close to a three-folded left-handed helical structure, with a rise per turn of 28.17 Å and a rise per disaccharide of 9.39 Å. For the HA/DMSD solution a very close minimum energy conformation was collected with 28.05 Å rise per turn and 9.35 Å rise per disaccharide unit revealing the absence of detectable influences of DMSD on HA three dimensional structure.

Earlier combined MD and NMR (solution) studies suggested that the preferential conformation of the HA molecule is close to the fourfolded helix form (code 2BVK and 1HUA in Fig. 4).[37,38] On the other hand crystallographic analyses have revealed that HA oligomers exhibit a regular helical conformation which can be depicted as left-handed helices, with three- or fourfolded periodicity.[40] It must be stated however that the conformation obtained experimentally is highly dependent on the experimental conditions.[41] Data from the literature shows that threefold and fourfold helices have been found under the largest range of conditions. The conformation obtained in the current study can be placed between a fourfold and a threefold periodicity, but closer to the three fold form. Thus, it is close to the structure with the PDB code 1HYA in Fig. 3 which was obtained in the presence of sodium ions through X-ray fiber diffraction (Winter, 1994). Other molecular modeling approaches revealed that the interconversion between the different helix shapes requires moderate conformational alterations of the glycosidic dihedral angles with low associated energy cost.[42]

CONCLUSIONS

The main ideas that emerge from the simulation of HA in the presence of DMSD suggest that the effects of dimethylsilanediol on HA conformation in aqueous solution are minor in low concentration regime. Several physical binding sites for DMSD were identified on the HA oligosaccharides the most active one being the carboxylate $–COO^-$ group of GlcUA. The DMSD was found to bind with slightly higher affinity than water at the exocyclic groups of HA showing the *same binding pattern* as the water molecules. Even the DMSD compete with water for the same HB sites it does not disrupt the water first hydration layer structure, due to the high water/DMSD ratio at the studied concentration (187:1) and pattern similarity. The self-interactions in HA, *i.e.* intra-molecular hydrogen bonding, was found not to be affected by the presence of DMSD. Thus, the conformations of HA extracted from the minimum energy glycosidic dihedrals were close to a three-folded left-handed helical structure for both HA and HA/DMSD systems. The results of the present study depict the DMSD-HA physical interaction as being weak at the concentrations usually used in pharmaceutical formulations and not affecting the three-dimensional conformation of HA in solution.

Acknowledgements: This research was financially suported by European Social Fund – "Cristofor I. Simionescu" Postdoctoral Fellowship Programme (ID POSDRU/89/1.5/S/55216), Sectoral Operational Programme Human Resources Development 2007 – 2013 and PN-II-ID-PCCE-2011-2-0028 contract grant number: 4/30.05.2012.

REFERENCES

1. R. Stern, *Clin. Dermatol.*, **2008**, *26*, 106-122.
2. R. Krasinski and H. Tchórzewski, *Postepy Hig. Med. Dosw*, **2007**, *61*, 683-689.
3. T. C. Laurent (Ed.), "The Chemistry, Biology, and Medical Applications of Hyaluronan and Its Derivatives", Portland Press: London, 1998, p. 305-314.
4. B. Weissman and K. Meyer, *J. Am. Chem. Soc.*, **1954**, *76*, 1753-1757.
5. A. J. Day and G. D. Prestwich, *J. Biol. Chem.*, **2002**, *277*, 4585-4588.
6. M. K. Cowman and S. Matsuoka, *Carbohydr. Res.*, **2005**, *340*, 791-809.
7. Y. Courbebaisse and M. C. Seguin, EP1750770A1, **2005**.
8. S. M. Sieburth, T. Nittoli, A. M. Mutahi and L. Guo, *Angew. Chem., Int. Ed.*, **1998**, *37*, 812-814.
9. C. A. Chen, S. M. Sieburth, A. Glekas, G. W. Hewitt, G. L. Trainor, S. Erickson-Viitanen, S. S. Garber, B. Cordova, S. Jeffry and R. M. Klabe, *Chem. Biol.*, **2001**, *8*, 1161-1166.
10. M. W. Mutahi, T. Nittoli, L. Guo and S. M. Sieburth, *J. Am. Chem. Soc.*, **2002**, *124*, 7363-7375.
11. S. M. Sieburth, C.A. Chen, *Eur. J. Org. Chem.*, **2006**, *2*, 311-322.
12. Y. M. Kim, S. Y. Farrah, R. H. Baney, *Electron. J. Biotechnol.*, **2006**, *9*, 176-181.
13. (a) S. Pronk, S. Páll, R. Schulz, P. Larsson, P. Bjelkmar, R. Apostolov, M. R. Shirts, J. C. Smith, P. M. Kasson, D. van der Spoel, B. Hess and E. Lindahl, *Bioinformatics*, **2013**, *29*, 845-854. (b) K. N. Kirschner, A. B. Yongye, S. M. Tschampel, J. González-Outeiriño, C. R. Daniels, B. L. Foley and R. J. Woods, *J. Comput. Chem.*, **2008**, *29*, 622-655.
14. H. W. Horn, W. C. Swope, J. W. Pitera, J. D. Madura, T. J. Dick, G. L. Hura and T. Head-Gordon, *J. Chem. Phys.*, **2004**, *120*, 9665-9679.
15. T. J. A. Ewing, S. Makino, A. G. Skillman and I. D. Kuntz, *J. Comput. Aided Molec. Design.*, **2001**, *15*, 411-428.
16. D. T. Moustakas, P.T. Lang, S. Pegg, E. T. Pettersen, I. D. Kuntz, N. Broojimans and R. C. Rizzo, *J. Comput. Aided Mol. Design*, **2006**, *20*, 601-609.

17. P.T. Lang, S. R. Brozell, S. Mukherjee, E. T. Pettersen, E. C. Meng, V. Thomas, R. C. Rizzo, D. A. Case, T. L. James and I. D. Kuntz, *RNA*, **2009**, *15*, 1219-1230.
18. C. I. Bayly, P. Cieplak, W. D. Cornell and P. A. Kollman, *J. Phys. Chem.*, **1993**, *97*, 10269-10280.
19. W. D. Cornell, P. Cieplak, C. I. Bayly, I. R. Gould, K. M. Merz, Jr., D. M. Ferguson, D. C. Spellmeyer, T. Fox, J. W. Caldwell and P. A. Kollman, *J. Am. Chem. Soc.*, **1995**, *117*, 5179-5197.
20. P. A. Kollman, *Acc. Chem. Res.*, **1996**, *29*, 461-469.
21. J. Wang and P. Cieplak, P. A. Kollman, *J. Comp. Chem.*, **2000**, *21*, 1049-1074.
22. Y. Duan, C. Wu, S. Chowdhury, M.C. Lee, G. Xiong, W. Zhang, R. Yang, P. Cieplak, R. Luo, T. Lee, J. Caldwell, J. Wang and P. Kollman, *J. Comp. Chem.*, **2003**, *24*, 1999-2012.
23. E. J. Sorin and V. S. Pande, *Biophys. J.*, **2005**, *88*, 2472-2493.
24. G. Bussi, D. Donadio and M. Parrinello, *J. Chem. Phys.*, **2007**, *126*, 014101-014108.
25. J. Černý and P. Hobza, *Phys. Chem. Chem. Phys.*, **2007**, ***9***, 5291-5303.
26. M. Rinaudo, *Macromol. Biosci.*, **2006**, *6*, 590-610.
27. D. van der Spoel, P. J. van Maaren, P. Larsson and N. Timneanu, *J. Phys. Chem. B*, **2006**, *110*, 4393-4398.
28. A. Almond, *Carbohydr. Res.*, **2005**, *340*, 907-920.
29. A. Luzar and D. Chandler, *Nature*, **1996**, *379*, 55-57.
30. Yu. I. Naberukhin and V. P Voloshin, *Z. Phys. Chem.*, **2009**, *223*, 1119-1131.
31. H. J. Bakker, J. J. Gilijamse and A. J. Lock, *Chem. Phys.Chem.*, **2005**, *6*, 1146-1156.
32. V. P. Voloshin and Yu. I. Naberukhin, *J. Struct. Chem.*, **2009**, *50*, 78-89.
33. O. Markovitch and N. Agmon, *J. Chem. Phys.*, **2008**, *129*, 084505-084518.
34. A. Luzar, *J. Chem. Phys.*, **2000**, *113*, 10663-10675.
35. A. Donati, A. Magnani, C. Bonechi, R. Barbucci and C. Rossi, *Biopolymers*, **2001**, *59*, 434-445.
36. A. Almond and J. K. Sheehan, *Glycobiology*, **2003**, *13*, 255-264.
37. A. Almond, P. L. DeAngelis and C. D. Blundell, *J. Mol. Biol.*, **2006**, *358i* 1256-1269.
38. S. M. Holmbeck, P. A. Petillo and L. E. Lerner, *Biochemistry*, **1994**, 33, 14246-14255.
39. W.T. Winter, P.J.C. Smith and Struther Arnott, *J. Mol. Biol.*, **1975**, *99*, 219-222.
40. E.D.T. Atkins, *Pure & Appl. Chem.*, **1977**, *49*, 1135-1149.
41. K. Haxaire, I. Braccini, M. Milas, M. Rinaudo and S. Pérez, *Glycobiology*, **2000**, *10*, 587-594.
42. J. K. Sheehan and E. D. T. Atkins, *Int. J. Biol. Macromol.*, **1983**, *5*, 215-221.